Journal of Statistics & Management Systems
ISSN 0972-0510 (Print), ISSN 2169-0014 (Online)
Vol. 29 (2026), No. 7 & 8, pp. 701–714
DOI : 10.47974/JSMS-1433

The new flexible Weibull-G family : Properties, simulations, and applications to COVID-19 data

Alexsandro A. Ferreira *
Gauss M. Cordeiro †
Department of Statistics
Universidade Federal de Pernambuco
Recife
Pernambuco
Brazil

Abstract

The flexible Weibull-G derives its properties from the exponentiated-G class. Its scope is expanded through a regression structure, with parameters estimated using maximum likelihood. Simulations confirm its consistency, and COVID-19 applications demonstrate superior performance compared to baseline models.

Subject Classification: *62E10, 62F10, 62P10.*

Keywords: *COVID-19, Flexible Weibull, Monte Carlo simulation, Newton-raphson.*

1. Introduction

Modeling complex phenomena poses a challenge for classical distributions such as Weibull and gamma, which are limited in their ability to accommodate non-monotonic hazard rate functions (hrf), such as bathtub or unimodal shapes. For this reason, the inclusion of additional parameters has been an effective strategy to increase the adaptability of models, resulting in the development of several families of generalized distributions in the literature, as evidenced by the works of [1], [2], [3], [4], [5], [6], [7], [8], [10], [11], [12], and [13], among many others.

The flexible Weibull (FW) distribution [14] for $\alpha, \beta > 0$ has cdf

$$G(x;\alpha,\beta) = 1 - \exp\left(-\mathrm{e}^{\alpha x - \frac{\beta}{x}}\right), \quad x > 0\,. \tag{1}$$

The new flexible Weibull-G (NFW-G) employs the transformed-transformer (T-X) [8] and (1). Thus, its cdf is (for $x \in \mathrm{IR}$)

* *E-mail:* **alexsandro.ferreira.aaf@gmail.com (Corresponding Author)**
† *E-mail:* **gauss@de.ufpe.br**

$$F(x,\alpha,\beta,\boldsymbol{\xi}) = 1 - \exp\left[-\exp\left(\alpha\{-\log[1-G(x;\boldsymbol{\xi})]\} - \frac{\beta}{\{-\log[1-G(x;\boldsymbol{\xi})]\}}\right)\right], \quad (2)$$

where $\boldsymbol{\xi}$ represents the parameter vector associated with $G(x)$. For notational simplicity, subsequent expressions suppress explicit parameter dependence in the functional forms. The corresponding probability density function (pdf) takes the form

$$\begin{aligned} f(x) &= \frac{g(x)}{1-G(x)}\left(\alpha + \frac{\beta}{\{-\log[1-G(x)]\}^2}\right) \\ &\quad \times \exp\left(\alpha\{-\log[1-G(x)]\} - \frac{\beta}{\{-\log[1-G(x)]\}}\right) \\ &\quad \times \exp\left[-\exp\left(\alpha\{-\log[1-G(x)]\} - \frac{\beta}{\{-\log[1-G(x)]\}}\right)\right], \; x \in \mathrm{IR}, \end{aligned} \quad (3)$$

where $g(x) = \mathrm{d}\,G(x)/\mathrm{d}x$. Consider a random variable X following the NFW-G distribution with density specified in (3). This structure is capable of generating various density and hrf configurations, including bimodal and bathtub-shaped patterns.

Section 2 presents three special models and their properties are detailed in Section 3, followed by a regression model in Section 4. The model's performance is then assessed via simulations (Section 5) and real-data applications (Section 6), with conclusions presented in Section 7.

2. Some NFW-G models

2.1 *New flexible Weibull Weibull (NFWW)*

The cdf of the Weibull baseline ($\lambda, \tau > 0$) is (for $x > 0$)

$$G(x) = 1 - \mathrm{e}^{-(x/\tau)^{\lambda}}.$$

The NFWW denisty arises from (3) as

$$\begin{aligned} f(x) &= \lambda\,\tau^{-\lambda}\,x^{\lambda-1}\left[\alpha + \beta(\tau/x)^{2\lambda}\right]\exp\left[\alpha(x/\tau)^{\lambda} - \beta(\tau/x)^{\lambda}\right] \\ &\quad \times \exp\left\{-\exp\left[\alpha(x/\tau)^{\lambda} - \beta(\tau/x)^{\lambda}\right]\right\}. \end{aligned} \quad (4)$$

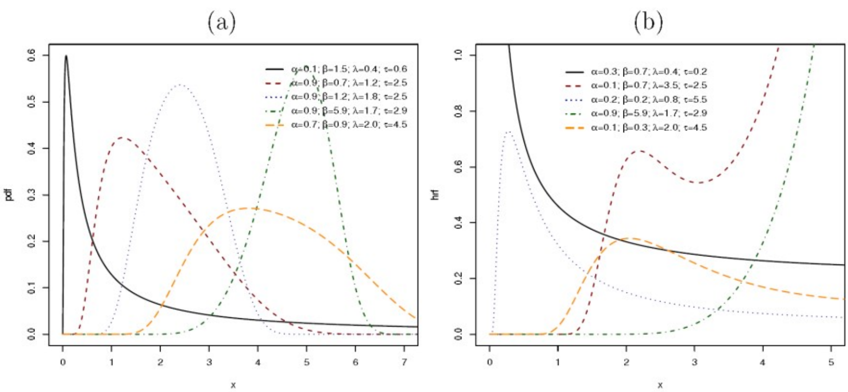

Figure 1
NFWW density and hrf.

2.2 *New flexible Weibull Kumaraswamy (NFWK)*

The Kumaraswamy cdf with parameters $a, b > 0$ is expressed by (for $0 < x < 1$)

$$G(x) = 1 - (1 - x^a)^b\,. \tag{5}$$

From (3) and (5), the density of the NFWK model reduces to

$$f(x) = \frac{a\,b\,x^{a-1}}{(1-x^a)}\left(\alpha + \frac{\beta}{[-b\log(1-x^a)]^2}\right)\exp\left(\alpha[-b\log(1-x^a)] - \frac{\beta}{[-b\log(1-x^a)]}\right)$$
$$\times \exp\left[-\exp\left(\alpha[-b\log(1-x^a)] - \frac{\beta}{[-b\log(1-x^a)]}\right)\right].$$

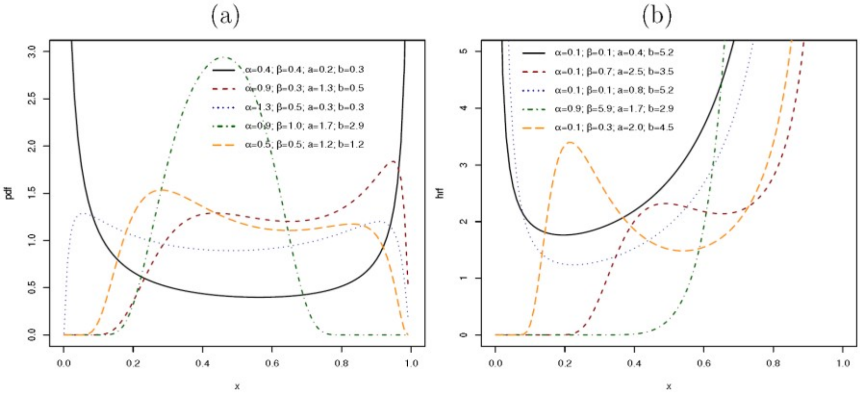

Figure 2
NFWK density and hrf.

2.3 *New flexible Weibull normal (NFWN)*

Applying (3) with the normal baseline $N(\mu, \sigma^2)$ (where $\mu \in \mathrm{IR}$ and $\sigma > 0$) yields the NFWN density as

$$f(x) = \frac{\phi(z)}{1-\Phi(z)}\left(\alpha + \frac{\beta}{\{-\log[1-\Phi(z)]\}^2}\right)$$
$$\times \exp\left(\alpha\{-\log[1-\Phi(z)]\} - \frac{\beta}{\{-\log[1-\Phi(z)]\}}\right)$$
$$\times \exp\left[-\exp\left(\alpha\{-\log[1-\Phi(z)]\} - \frac{\beta}{\{-\log[1-\Phi(z)]\}}\right)\right],$$

where $z = (x - \mu)/\sigma$, and $\phi(\cdot)$ and $\Phi(\cdot)$ are the pdf and cdf of the standard normal, respectively.

The pdfs and hrfs of the special models appear in Figures 1, 2, and 3. The proposed distributions capture various data structures, from right-skewed to symmetric and left-skewed, while their hrfs exhibit unimodal, increasing-decreasing-increasing, and bathtub shapes.

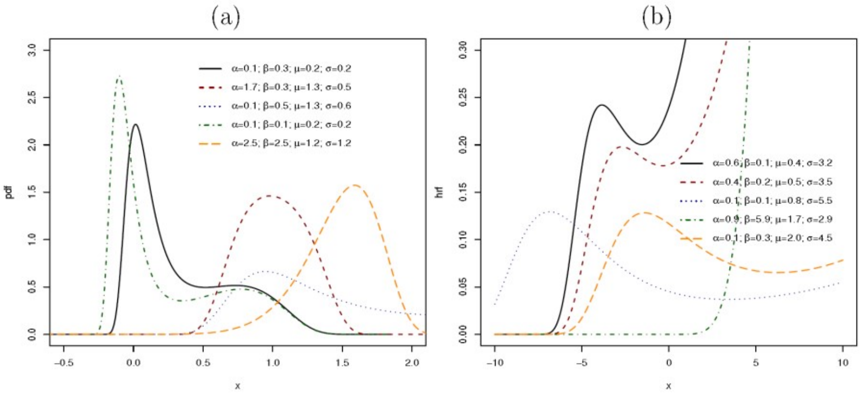

Figure 3
NFWN density and hrf.

3. Mathematical Results

3.1 *Useful expansions*

Consider the power series expansion

$$\exp(-z) = \sum_{k=0}^{\infty} \frac{(-1)^k}{k!} z^k \,. \tag{6}$$

Under conditions $|v| < 1$ and $q \in \mathrm{IR}$, the generalized binomial expansion becomes

$$(1-v)^{-q} = \sum_{j=0}^{\infty} (-1)^j \binom{-q}{j} v^j \,, \tag{7}$$

where $\binom{-q}{0} = 1$ and $\binom{-q}{j} = \frac{1}{j!} \prod_{n=1}^{j} (-q-n+1)$ (for $j \geq 1$). Then, applying (6) in (2),

$$F(x) = \sum_{i=1}^{\infty} \frac{(-1)^{i+1}}{i!} \exp(i\alpha\{-\log[1-G(x)]\}) \exp\left(-\frac{i\beta}{\{-\log[1-G(x)]\}}\right) . \tag{8}$$

Next, using (7),

$$\exp(i\alpha\{-\log[1-G(x)]\}) = [1-G(x)]^{-i\alpha} = \sum_{j=0}^{\infty} (-1)^j \binom{-i\alpha}{j} G(x)^j \,. \tag{9}$$

Further, the Taylor expansion of $[-\log(1-w)]^{-1}$ at $w=0$ gives

$$[-\log(1-w)]^{-1} = \frac{1}{w} + \sum_{\ell=0}^{\infty} a_\ell \, w^{\ell} \,, \tag{10}$$

where $a_0 = -1/2$, $a_1 = -1/12$, $a_2 = -1/24$, $a_3 = -19/720$, $a_4 = -3/160$, etc.

Applying (10) to the last exponential function in (8),

$$\exp\left(-\frac{i\beta}{\{-\log[1-G(x)]\}}\right) = \exp\left[-i\beta\left(\frac{1}{G(x)} + \sum_{k=0}^{\infty} a_k \, G(x)^k\right)\right] . \tag{11}$$

A power series for $1/G(x)$ can be found by applying (7) since $G(x) \in (0,1)$ as

$$\frac{1}{1-[1-G(x)]} = \sum_{\ell=0}^{\infty} [1-G(x)]^{\ell} = \sum_{\ell=0}^{\infty} \sum_{k=0}^{\ell} (-1)^k \binom{\ell}{k} G(x)^k = \sum_{k=0}^{\infty} b_k \, G(x)^k \,, \tag{12}$$

where

$$b_k = \sum_{\ell=k}^{\infty} (-1)^k \binom{\ell}{k} .$$

Thus, employing (12) in (11),

$$\exp\left(-\frac{i\beta}{\{-\log[1-G(x)]\}}\right) = \exp(\sum_{k=0}^{\infty} c_k \, G(x)^k) \,,$$

where $c_k = -i\beta(b_k + a_k)$. Then, Theorem 25 of [15] leads to

$$\exp\left(-\frac{i\beta}{\{-\log[1-G(x)]\}}\right) = \sum_{k=0}^{\infty} d_k \, G(x)^k \,, \tag{13}$$

where $d_0 = \exp(c_0)$ and $d_k = (1/k) \sum_{m=1}^{k} m \, c_m \, d_{k-m}$ for $k \geq 1$. Thus, using the results obtained in (9) and (13) in Equation (8),

$$F(x) = \sum_{j,k=0}^{\infty} \varphi_{j,k} \, G(x)^{j+k} \,, \tag{14}$$

where

$$\varphi_{j,k} = \varphi_{j,k}(\alpha,\beta) = (-1)^j \binom{-i\alpha}{j} d_k .$$

By differentiating (14), the NFW-G density becomes

$$f(x) = \sum_{\substack{j,k=0 \\ j+k>0}}^{\infty} \varphi_{j,k} \, \pi_{j+k}(x) \,, \tag{15}$$

where $\pi_{j+k}(x)$ denotes the exp-G density with power $j+k$. Equation (15) relates NFW-G properties to the exp-G class.

Figure 4 displays NFWW Bonferroni and Lorenz curves for selected α and β values ($\tau = 0.1$, $\lambda = 0.3$).

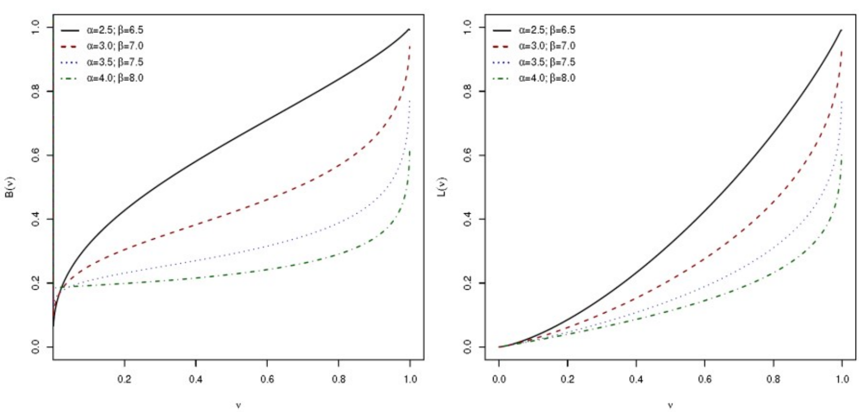

Figure 4
NFWW($\boldsymbol{\alpha, \beta, \tau, \lambda}$) Bonferroni and Lorenz curves.

3.2 *Estimation*

Suppose $x_1, \ldots, x_n$ represent independent realizations from the NFW-G. The log-likelihood corresponding to $\boldsymbol{\theta} = (\alpha, \beta, \boldsymbol{\xi})^T$ is

$$\ell(\boldsymbol{\theta}) = \sum_{i=1}^{n} (\log g(x_i) - \log[1 - G(x_i)]) + \sum_{i=1}^{n} \log\left(\alpha + \frac{\beta}{\{-\log[1-G(x_i)]\}^2}\right)$$
$$+ \sum_{i=1}^{n} \left(\alpha\{-\log[1 - G(x_i)]\} - \frac{\beta}{\{-\log[1-G(x_i)]\}}\right)$$
$$+ \sum_{i=1}^{n} \left[-\exp\left(\alpha\{-\log[1 - G(x_i)]\} - \frac{\beta}{\{-\log[1-G(x_i)]\}}\right)\right]. \tag{16}$$

Parameter estimates follow from numerically optimizing Equation (16).

4. The regression model

Given X with pdf (4), $Y = \log(X)$ follows the LNFWW density with $\tau = \mathrm{e}^{\mu}$ and $\lambda = 1/\sigma$ ($y \in \mathrm{IR}$) in the form

$$f(y) = \frac{1}{\sigma}\,\mathrm{e}^{\left(\frac{y-\mu}{\sigma}\right)}\left[\alpha + \beta\,\mathrm{e}^{-2\left(\frac{y-\mu}{\sigma}\right)}\right]\exp\left[\alpha\,\mathrm{e}^{\left(\frac{y-\mu}{\sigma}\right)} - \beta\,\mathrm{e}^{-\left(\frac{y-\mu}{\sigma}\right)}\right]$$
$$\exp\left[-\mathrm{e}^{\alpha\,\mathrm{e}^{\left(\frac{y-\mu}{\sigma}\right)} - \beta\,\mathrm{e}^{-\left(\frac{y-\mu}{\sigma}\right)}}\right], \tag{17}$$

under constraints $\alpha, \beta, \sigma > 0$ and $\mu \in \mathrm{IR}$. Application of the transformation $Z = (y - \mu)/\sigma$ results in the density

$$f(z) = \mathrm{e}^{z}[\alpha + \beta \mathrm{e}^{-2z}]\exp[\alpha\,\mathrm{e}^{z} - \beta\,\mathrm{e}^{-z}]\exp\left[-\mathrm{e}^{\alpha\,\mathrm{e}^{z} - \beta\,\mathrm{e}^{-z}}\right],\ z \in \mathrm{IR}. \tag{18}$$

Equation (18) represents the standard LNFWW density. For response y_i and covariates $\mathbf{v}_i^T = (v_{i1}, \cdots, v_{ip})^T$, the regression model becomes

$$y_i = \mathbf{v}_i^T \boldsymbol{\eta} + \sigma z_i\,, \quad i = 1, \ldots, n\,, \tag{19}$$

where $\mu_i = \mathbf{v}_i^T \boldsymbol{\eta}$ for coefficient vector $\boldsymbol{\eta} = (\eta_1, \cdots, \eta_p)^T$ and z_i: (18).

Combining expressions (18) and (19), the log-likelihood function with respect to $\boldsymbol{\zeta} = (\alpha, \beta, \sigma, \boldsymbol{\eta}^T)^T$ takes the form below. Here, each observed value y_i represents the minimum between lifetime Y_i and censoring time C_i, which arise independently. The resulting log-likelihood equals

$$\ell(\boldsymbol{\zeta}) = -d\log(\sigma) + \sum_{i\in F} z_i + \sum_{i\in F}\log[\alpha + \beta \mathrm{e}^{-2z_i}] + \alpha\sum_{i\in F}\mathrm{e}^{z_i} -$$
$$\beta\sum_{i\in F}\mathrm{e}^{-z_i} + \sum_{i\in F}\left[-\mathrm{e}^{\alpha\,\mathrm{e}^{z_i} - \beta\,\mathrm{e}^{-z_i}}\right] + \sum_{i\in C}\left[-\mathrm{e}^{\alpha\,\mathrm{e}^{z_i} - \beta\,\mathrm{e}^{-z_i}}\right], \tag{20}$$

where d counts complete observations, $z_i = (y_i - \mu_i)/\sigma$, and indicator sets F and C distinguish between event times and censored values. Numerical maximization of (20) produces $\hat{\boldsymbol{\zeta}}$.

5. Simulations

The performance of the maximum likelihood estimate (MLE) in three NFWW parameter scenarios uses samples of $n = 50{,}100{,}200{,}500$ generated using the Newton-Raphson method. In over 1,000 Monte Carlo runs, average estimates (AEs), biases, and mean squared errors (MSEs) are calculated using BFGS in optim within R for $\boldsymbol{\theta} = (\alpha, \beta, \tau, \lambda)^T$.

Table 1
Investigation of the NFWW via Simulation.

		(0.7, 0.9, 2.5, 0.5)			(1.5, 1.2, 1.8, 0.5)			(2.9, 0.6, 0.4, 0.8)		
n	$\boldsymbol{\theta}$	AE	Bias	MSE	AE	Bias	MSE	AE	Bias	MSE
50	α	0.7401	0.0401	0.3089	1.7037	0.2037	2.8204	2.9618	0.0618	1.3594
	β	0.9101	0.0101	0.4027	1.4021	0.2021	2.7186	0.7273	0.1273	0.9283
	τ	2.5748	0.0748	0.1551	1.7898	-0.0101	0.0831	0.3772	-0.0227	0.0041
	λ	0.5767	0.0767	0.0441	0.6356	0.1356	0.1112	1.0219	0.2219	0.2696
100	α	0.7047	0.0047	0.0705	1.6616	0.1616	1.4052	3.0297	0.1297	0.8642
	β	0.8896	-0.0103	0.1159	1.3352	0.1352	1.2802	0.7080	0.1080	0.5440
	τ	2.5480	0.0480	0.1004	1.8512	0.0512	0.1053	0.3958	-0.0041	0.0019
	λ	0.5419	0.0419	0.0196	0.5686	0.0686	0.0504	0.9110	0.1110	0.1229
200	α	0.6959	-0.0040	0.0285	1.5391	0.0391	0.3537	2.9492	0.0492	0.3358
	β	0.8841	-0.0158	0.0498	1.2228	0.0228	0.2750	0.6329	0.0329	0.1526
	τ	2.5381	0.0381	0.0533	1.8269	0.0269	0.0475	0.4003	0.0003	0.0016
	λ	0.5226	0.0226	0.0083	0.5373	0.0373	0.0222	0.8585	0.0585	0.0548
500	α	0.6975	-0.0024	0.0116	1.5093	0.0093	0.1013	2.9300	0.0300	0.1075
	β	0.8929	-0.0070	0.0182	1.2017	0.0017	0.0708	0.6047	0.0047	0.0386
	τ	2.5190	0.0190	0.0386	1.8161	0.0161	0.0262	0.4028	0.0028	0.0007
	λ	0.5096	0.0096	0.0032	0.5157	0.0157	0.0085	0.8246	0.0246	0.0211

The Newton-Raphson iterative method is used to generate random variates from the NFWW, as outlined in the steps below

1. Set the model parameters $\alpha, \beta, \tau, \lambda$ and an initial value x^0.
2. Generate $u \sim$Uniform (0,1).
3. Update the iterative value x^* using

$$x^* = x^0 - \frac{F(x^0; \alpha, \beta, \tau, \lambda) - u}{f(x^0; \alpha, \beta, \tau, \lambda)},,$$

   where $F(\cdot)$ and $f(\cdot)$ denote the cdf (2) and pdf (4), respectively.
4. Repeat step 3 until $|x^0 - x^*| < \varepsilon$, where ε is a small tolerance. Upon convergence, set $x^0 = x^*$ as the generated NFWW variate.
5. Repeat steps 2–4 n times to obtain n independent NFWW samples.

Table 1 confirms MLE consistency: biases and MSEs vanish as n increases. For (0.7, 0.9, 2.5, 0.5), α bias and MSE drop from 0.0401 to 0.0024 and 0.3089 to 0.0116 (n: 50 to 500). Other parameters show similar patterns.

Table 2
Investigation of the LNFWW via Simulation.

		0%			10%			30%		
n	ζ	AE	Bias	MSE	AE	Bias	MSE	AE	Bias	MSE
50	α	0.5911	-0.0088	0.0728	0.5965	-0.0034	0.0758	0.6245	0.0245	0.1898
	β	0.4915	-0.0084	0.0887	0.4911	-0.0088	0.0903	0.5182	0.0182	0.1036
	σ	2.3917	-0.1082	0.6176	2.3930	-0.1069	0.6617	2.4667	-0.0332	0.8158
	η_0	0.7812	-0.0187	0.0370	0.7856	-0.0143	0.0350	0.7814	-0.0185	0.0449
	η_1	1.5841	-0.0158	0.0262	1.5878	-0.0121	0.0248	1.5844	-0.0155	0.0318
100	α	0.5959	-0.0040	0.0252	0.6142	0.0142	0.0354	0.6196	0.0196	0.0761
	β	0.5045	0.0045	0.0427	0.4964	-0.0035	0.0421	0.4998	-0.0001	0.0421
	σ	2.4631	-0.0368	0.2691	2.4650	-0.0349	0.2818	2.4847	-0.0152	0.3201
	η_0	0.7849	-0.0150	0.0195	0.8114	0.0114	0.0261	0.8195	0.0195	0.0369
	η_1	1.5872	-0.0127	0.0138	1.6096	0.0096	0.0184	1.6164	0.0164	0.0261
200	α	0.5985	-0.0014	0.0133	0.5934	-0.0065	0.0143	0.5952	-0.0047	0.0370
	β	0.5023	0.0023	0.0173	0.5061	0.0061	0.0176	0.5066	0.0066	0.0183
	σ	2.4802	-0.0197	0.1189	2.4813	-0.0186	0.1266	2.4882	-0.0117	0.1445
	η_0	0.7919	-0.0080	0.0098	0.7803	-0.0196	0.0079	0.7858	-0.0141	0.0166
	η_1	1.5931	-0.0068	0.0069	1.5834	-0.0165	0.0056	1.5880	-0.0119	0.0118
500	α	0.5945	-0.0054	0.0061	0.6024	0.0024	0.0084	0.6020	0.0020	0.0141
	β	0.4976	-0.0023	0.0067	0.4937	-0.0062	0.0074	0.4941	-0.0058	0.0076
	σ	2.4766	-0.0233	0.0465	2.4790	-0.0209	0.0485	2.4805	-0.0194	0.0528
	η_0	0.7919	-0.0080	0.0086	0.8070	0.0070	0.0139	0.8076	0.0076	0.0177
	η_1	1.5931	-0.0068	0.0061	1.6058	0.0058	0.0098	1.6064	0.0064	0.0125

Over 1,000 Monte Carlo runs, regression MLEs use samples ($n = 50,100,200,500$) via acceptance-rejection with $\alpha = 0.6, \beta = 0.5, \sigma = 2.5, \eta_0 = 0.8, \eta_1 = 1.6$. Censoring times from uniform$(0, b)$ yield 0%, 10%, or 30% censoring. Nelder-Mead in R maximizes (20) from true parameter starts.

The simulation scheme proceeds as follows for $i = 1,2, \dots, n$:

1. Draw $v_{i1} \sim$ Uniform $(0,1)$ and compute $\mu_i = \eta_0 + \eta_1 v_{i1}$.
2. Sample t_i from the density $w(t_i) = (1/\sigma)\exp\{(t_i - \mu_i)/\sigma - \exp[(t_i - \mu_i)/\sigma]\}$.
3. Generate $u \sim$ Uniform $(0,1)$.
4. Accept t_i as y_i if $u \leq f(t_i)/(Mw(t_i))$, where $f(\cdot)$ refers to (17) and (19), and $M = \max[f(t_i)/w(t_i)]$, otherwise, return to Step 3.
5. Draw $c_i \sim \text{Uniform}(0, b)$.
6. Define the censoring indicator as $\delta_i = 1$ if $y_i \leq c_i$, and $\delta_i = 0$ otherwise. The observed time is then $y_i^* = \min(y_i, c_i)$.

Table 2 establishes MLE consistency: biases and MSEs vanish as n increases. For α (0% censoring), bias drops from 0.0088 to 0.0054 and MSE from 0.0728 to 0.0061 (n: 50 to 500). Other parameters and censoring scenarios exhibit similar behavior, confirming precision under censoring.

6. Applications

The NFWW model's empirical performance receives evaluation through two COVID-19 data sets. Competing distributions include Kumaraswamy Weibull (KW) [16], beta-Weibull (BW) [17], Weibull Weibull (WW) [9], Lomax Weibull (LW) [18], and Weibull (WE) models. Goodness-of-fit evaluation combines Cramér-von Mises (W^*) and Anderson-Darling (A^*) test statistics [19] with information criteria including AIC (Akaike), CAIC (Consistent Akaike), BIC (Bayesian), and HQIC (Hannan-Quinn). The Kolmogorov-Smirnov (KS) statistic and corresponding p -value complement this assessment framework.

6.1 *COVID-19 data in Pakistan*

The NFWW distribution is applied to daily confirmed COVID-19 cases in Pakistan (March 21–May 29, 2020) [20], comprising 70 observations. Comparative assessment against the competing models evaluates NFWW performance.

Tables 3–4 report MLEs and their standard errors (SEs) (in parentheses) via AdequacyModel [21] and fit statistics, confirming NFWW superiority. The generalized likelihood ratio (GLR) tests [22] against KW, BW, WW, LW, and WE yield values 12.346, 14.959, 8.651, 17.532, and 37.372, establishing NFWW optimality. Figure 5 confirms NFWW (solid line) superiority over KW and LW through fitted pdfs and cdfs.

Table 3

Model parameter estimates and SEs.

Model	MLEs (SEs)			
NFWW$(\alpha,\beta,\tau,\lambda)$	0.044	15.264	9.875	0.639
	(0.005)	(1.919)	(0.014)	(0.004)
KW(a,b,τ,λ)	36.381	0.066	0.578	5.409
	(0.089)	(0.008)	(0.002)	(0.003)
BW(a,b,τ,λ)	54.570	0.061	0.463	1.114
	(26.966)	(0.008)	(0.002)	(0.005)
WW$(\alpha,\beta,\tau,\lambda)$	0.007	1.607	0.239	8.429
	(0.005)	(1.886)	(0.048)	(37.597)
LW$(\alpha,\beta,\tau,\lambda)$	0.062	19.471	0.529	2.953
	(0.008)	(9.645)	(0.004)	(0.012)
WE(τ,λ)	20.101	0.226		
	(5.262)	(0.023)		

Table 4
Adequacy measures for COVID-19 data in Pakistan

Model	W^*	A^*	AIC	CAIC	BIC	HQIC	KS	p-value
NFWW	0.124	0.816	1095.009	1095.624	1104.003	1098.581	0.104	0.401
KW	0.193	1.241	1116.629	1117.245	1125.623	1120.202	0.121	0.233
BW	0.201	1.295	1135.247	1135.863	1144.241	1138.820	0.180	0.017
WW	0.163	1.100	1104.369	1104.985	1113.363	1107.942	0.097	0.488
LW	0.190	1.239	1132.542	1133.157	1141.536	1136.114	0.180	0.018
WE	0.204	1.334	1316.354	1316.533	1320.851	1318.140	0.753	< 0.001

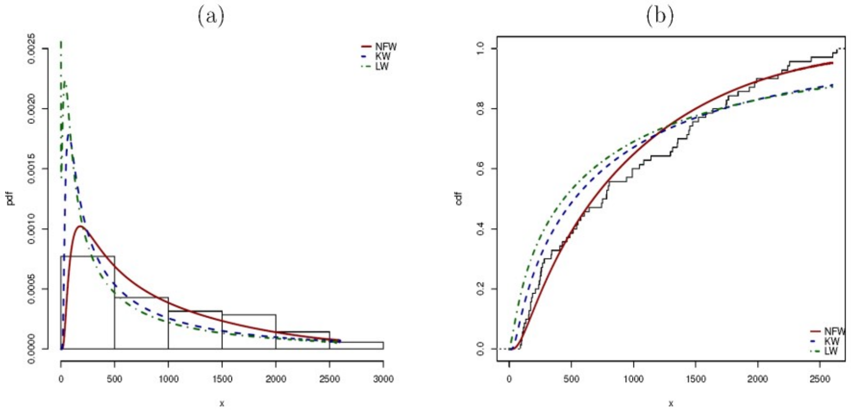

Figure 5
Pdfs and cdfs for COVID-19 data in Pakistan.

6.2 *COVID-19 data in Ceará*

Data from https://github.com/integrasus/api-covid-ce contain 368 COVID-19 lifetimes (in days, Ceará, Brazil, 2021-2022) with y_i representing symptom-to-death duration.

Approximately 50% of observations are censored (non-COVID deaths or survivors). Covariates include: δ_i (censoring: 0 = censored, 1 = observed lifetime), v_{i1} (age in years), and v_{i2} (immunodeficiency: 1 = yes, 0 = no).

Figure 6 displays (a) mortality peaking near age 60 and (b) reduced survival among immunodeficient patients.

Then,

$$y_i = \eta_0 + \eta_1 v_{i1} + \eta_2 v_{i2} + \sigma z_i, \qquad i = 1, \dots, 368\,,$$

where z_i has pdf (18). Results are compared against log-Kumaraswamy Weibull (LKW) and log-beta Weibull (LBW) regressions. Table 5 reports MLEs (SEs in parentheses, p-values in brackets) obtained via conjugate gradient CG in optim for Equation (20). Age and immunodeficiency prove significant at 5%, with negative η_1 and η_2 indicating reduced survival for older or immunodeficient individuals.

LNFWW yields lowest fit statistics (Table 6) and dominates via GLR tests (LKW: 60.168, LBW: 46.093). Quantile residuals [23] assess fit in the form

$$qr_i = \Phi^{-1}\left(1 - \exp\left\{-\exp\left[\hat{\alpha}\, e^{\hat{z}_i} - \hat{\beta}\, e^{-\hat{z}_i}\right]\right\}\right),$$

where $\hat{z}_i = (y_i - \hat{\mu}_i)/\hat{\sigma}$, with $\hat{\mu}_i = \mathbf{v}_i^T \hat{\boldsymbol{\eta}}$ and $\Phi^{-1}(\cdot)$ denoting the standard normal quantile function, Figure 7 shows qrs approximating normality, confirming the adequacy of the LNFWW fit.

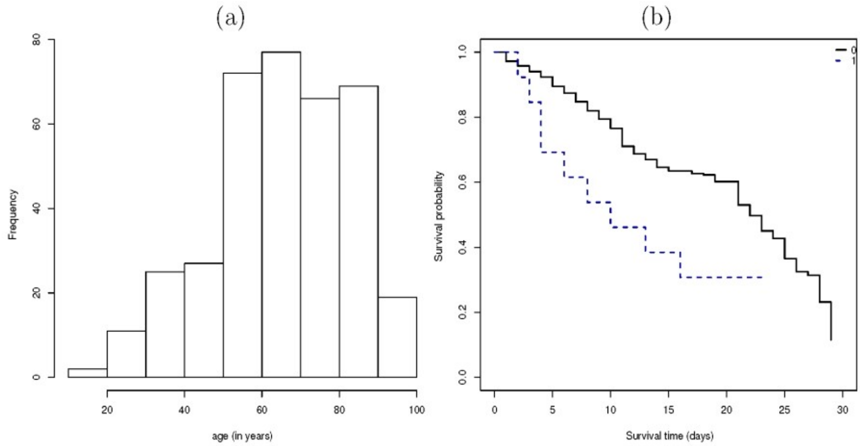

Figure 6
(a) Age histogram and (b) Kaplan-Meier curves for immunodeficiency.

Table 5
Results for COVID-19 data in Ceará.

Model	α	β	σ	η_0	η_1	η_2
LNFWW	1.196	6.526	3.761	1.531	-0.021	-0.504
	(0.429)	(1.735)	(1.360)	(0.472)	(0.003)	(0.231)
				[0.003]	[< 0.001]	[0.029]
LKW	3.597	1.822	1.652	4.160	-0.023	-0.773
	(1.929)	(0.838)	(0.566)	(0.187)	(0.003)	(0.264)
				[< 0.001]	[< 0.001]	[0.003]
LBW	1.743	1.423	0.882	4.825	-0.024	-0.647
	(0.383)	(0.734)	(0.101)	(0.462)	(0.003)	(0.217)
				[< 0.001]	[< 0.001]	[0.003]

Table 6
Adequacy measures for COVID-19 data in CearÃ¡.

Model	AIC	CAIC	BIC	HQIC
LFWW	718.713	719.114	742.161	728.029
LKW	725.993	726.394	749.442	735.309
LBW	727.351	727.752	750.800	736.667

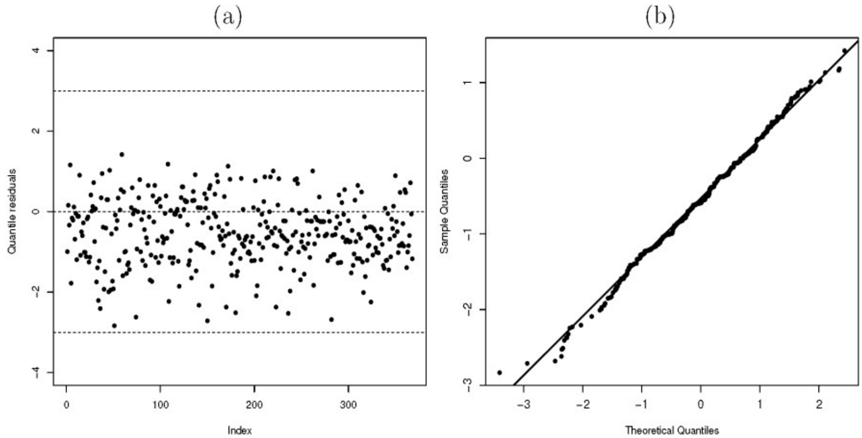

Figure 7
(a) Index and (b) normal plots of qrs for Ceará COVID-19.

Conclusions

This paper introduced the flexible Weibull-G family, deriving properties from the exponentiated-G class, and developed an associated regression model. Simulations established MLE consistency, while COVID-19 applications demonstrated superiority over competing models. Future research may explore alternative regression specifications, Bayesian inference, and applications across diverse domains.

Acknowledgments

Fundação de Amparo á Ciência e Tecnologia do Estado de Pernambuco (FACEPE) [IBPG-1448-1.02/20] supports this work.

References

[1] A. W. Marshall and I. Olkin, "A new method for adding a parameter to a family of distributions with application to the exponential and Weibull families," *Biometrika,* vol. 84, pp. 641–652 (1997).

[2] R. C. Gupta, P. L. Gupta, and R. D. Gupta, "Modeling failure time data by Lehmann alternatives," *Communications in Statistics - Theory and Methods,* vol. 27, pp. 887–904 (1998).

[3] N. Eugene, C. Lee, and F. Famoye, "Beta-normal distribution and its applications," *Communications in Statistics - Theory and Methods,* vol. 31, pp. 497–512 (2002).

[4] K. Zografos and N. Balakrishnan, “On families of beta- and generalized gamma-generated distributions and associated inference,” *Statistical Methodology*, vol. 6, pp. 344–362 (2009).

[5] G. M. Cordeiro and M. de Castro, “A new family of generalized distributions,” *Journal of Statistical Computation and Simulation*, vol. 81, pp. 883–898 (2011).

[6] C. Alexander, G. M. Cordeiro, E. M. M. Ortega, and J. Sarabia, “Generalized beta-generated distributions,” *Computational Statistics & Data Analysis*, vol. 56, pp. 1880–1897 (2012).

[7] G. M. Cordeiro, E. M. M. Ortega, and D. C. C. Cunha, “The exponentiated generalized class of distributions,” *Journal of Data Science,* vol. 11, pp. 1–27 (2013).

[8] A. Alzaatreh, C. Lee, and F. Famoye, “A new method for generating families of continuous distributions,” *METRON*, vol. 71, pp. 63–79 (2013).

[9] M. Bourguignon, R. Silva, and G. M. Cordeiro, “The Weibull-G family of probability distributions,” *Journal of Data Science*, vol. 12, pp. 53–68 (2014).

[10] M. Alizadeh, M. Emadi, M. Doostparast, G. M. Cordeiro, E. M. M. Ortega, and R. R. Pescim, “A new family of distributions: the Kumaraswamy odd log-logistic, properties and applications,” *Hacettepe Journal of Mathematics and Statistics,* vol. 44, pp. 1491–1512 (2015).

[11] F. Chipepa, B. O. Oluyede, and B. Makubate, “A new generalized family of odd Lindley-G distributions with application,” *International Journal of Statistics and Probability*, vol. 8, pp. 1–22 (2019).

[12] L. A. Baharith and H. H. Alamoudi, “The exponentiated Fréchet generator of distributions with applications,” *Symmetry,* vol. 13, p. 572 (2021).

[13] B. P. Tlhaloganyang, W. Sengweni, and B. Oluyede, “The gamma odd Burr X-G family of distributions with applications,” *Pakistan Journal of Statistics and Operation Research*, vol. 18, pp. 721–746 (2022).

[14] M. Bebbington, C.-D. Lai, and R. Zitikis, “A flexible Weibull extension,” *Reliability Engineering & System Safety*, vol. 92, pp. 719–726 (2007).

[15] A. U. K. M. Munir, “Series representations and approximation of some quantile functions appearing in finance,” Ph.D. dissertation, Dept. Mathematics, University College London (2013).

[16] G. M. Cordeiro, E. M. M. Ortega, and S. Nadarajah, "The Kumaraswamy Weibull distribution with application to failure data," *Journal of the Franklin Institute*, vol. 347, pp. 1399–1429 (2010).

[17] C. Lee, F. Famoye, and O. Olumolade, "Beta-Weibull distribution: Some properties and applications to censored data," *Journal of Modern Applied Statistical Methods*, vol. 6, p. 17 (2007).

[18] G. M. Cordeiro, A. Z. Afify, E. M. M. Ortega, A. K. Suzuki, and M. E. Mead, "The odd Lomax generator of distributions: Properties, estimation and applications," *Journal of Computational and Applied Mathematics*, vol. 347, pp. 222–237 (2019).

[19] G. Chen and N. Balakrishnan, "A general purpose approximate goodness-of-fit test," *Journal of Quality Technology*, vol. 27, pp. 154–161 (1995).

[20] R. A. R. Bantan, C. Chesneau, F. Jamal, and M. Elgarhy, "On the analysis of new COVID-19 cases in Pakistan using an exponentiated version of the M family of distributions," *Mathematics*, vol. 8, p. 953 (2020).

[21] P. R. D. Marinho, R. B. Silva, M. Bourguignon, G. M. Cordeiro, and S. Nadarajah, "AdequacyModel: An R package for probability distributions and general purpose optimization," *PLOS ONE*, vol. 14, pp. 1–30 (2019).

[22] Q. H. Vuong, "Likelihood ratio tests for model selection and non-nested hypotheses," *Econometrica*, vol. 57, pp. 307–333 (1989).

[23] P. K. Dunn and G. K. Smyth, "Randomized quantile residuals," *Journal of Computational and Graphical Statistics*, vol. 5, pp. 236–244 (1996).

Received August, 2024